Acta Crystallographica Section D
Biological Crystallography
ISSN 1399-0047

Unprecedented conformational flexibility revealed in the ligand-binding domains of the *Bovicola ovis* ecdysone receptor (EcR) and ultraspiracle (USP) subunits

Bin Ren,[a]*‡ Thomas S. Peat,[a] Victor A. Streltsov,[a] Matthew Pollard,[b] Ross Fernley,[a] Julian Grusovin,[a] Shane Seabrook,[a] Pat Pilling,[a] Tram Phan,[a] Louis Lu,[a] George O. Lovrecz,[a] Lloyd D. Graham[b] and Ronald J. Hill[b]*§

[a]CSIRO Materials Science and Engineering, 343 Royal Parade, Parkville, VIC 3052, Australia, and [b]CSIRO Animal, Food and Health Sciences, PO Box 52, North Ryde, NSW 1670, Australia

‡ Correspondence regarding crystallography should be addressed to this author.
§ Correspondence regarding biology should be addressed to this author.

Correspondence e-mail: bin.ren@csiro.au, ron.hill@csiro.au

Received 28 March 2014
Accepted 28 April 2014

PDB references: BoEcR–BoUSP, co-crystallized with methylene lactam, 4ozr; complex with ponasterone A, 4ozt

The heterodimeric ligand-binding region of the *Bovicola ovis* ecdysone receptor has been crystallized either in the presence of an ecdysteroid or a synthetic methylene lactam insecticide. Two X-ray crystallographic structures, determined at 2.7 Å resolution, show that the ligand-binding domains of both subunits of this receptor, like those of other nuclear receptors, can display significant conformational flexibility. Thermal melt experiments show that while ponasterone A stabilizes the higher order structure of the heterodimer in solution, the methylene lactam destabilizes it. The conformations of the EcR and USP subunits observed in the structure crystallized in the presence of the methylene lactam have not been seen previously in any ecdysone receptor structure and represent a new level of conformational flexibility for these important receptors. Interestingly, the new USP conformation presents an open, unoccupied ligand-binding pocket.

1. Introduction

The 1950s saw the first isolation of a hormone termed ecdysone, which was active in promoting the moulting of insects (Butenandt & Karlson, 1954). Subsequently, a more polar and generally biologically more active form, 20-hydroxyecdysone, was isolated from insects and also from crustacea (Karlson, 1956; Horn & Bergamasco, 1985). However, it was not until the 1990s that the first receptor for ecdysteroid hormones was isolated and characterized as a heterodimer of the nuclear receptor proteins EcR and USP (Koelle *et al.*, 1991; Yao *et al.*, 1992, 1993; Thomas *et al.*, 1993). In addition to their central role in regulating the expression of hundreds of genes during arthropod development, ecdysone receptors provide an intriguing target for the control of insect populations as these proteins vary significantly between arthropod taxa and are absent from vertebrates. Indeed, several classes of synthetic insecticidal chemistries targeting ecdysone receptors have been discovered, including the bisacylhydrazines (Wing *et al.*, 1988) and methylene lactams (Birru *et al.*, 2010). Members of the bisacylhydrazine class, which are selective for Lepidoptera, have been brought to market on the basis of safety and environmental friendliness (Dhadialla *et al.*, 1998; Nakagawa, 2005).

The binding of ecdysteroids to the ligand-binding domain (LBD) of the EcR subunit of ecdysone receptors has been established and well characterized (Koelle *et al.*, 1991; Hu *et al.*, 2003; Graham, Johnson *et al.*, 2007). However, the ligand-binding status of the more evolutionarily variable USP subunit

has been more controversial and clearly is not as simple (for reviews, see Hill *et al.*, 2013; Jindra *et al.*, 2013; Jones, Jones *et al.*, 2013). In the basal insect order Orthoptera, USP binds 9-*cis*-retinoic acid and thus behaves like a vertebrate retinoid X receptor (RXR; Nowickyj *et al.*, 2008). In Coleoptera and Hemiptera it has been suggested that USP is unable to bind ligands and simply acts as a constitutive structural partner for EcR (Iwema *et al.*, 2007). However, one research group has long postulated that, at least in the case of the mecopteran *Drosophila melanogaster*, USP binds a sesquiterpenoid related to juvenile hormone (initially proposed to be juvenile hormone III or juvenile hormone III acid and more recently to be methyl farnesoate) as a functional step on a pathway of physiological and developmental significance (Jones & Sharp, 1997; Jones, Teal *et al.*, 2013).

The LBDs of nuclear receptors typically comprise 12 α-helices (H1–H12) arranged in a three-layer sandwich with a β-sheet in the loop between helices H5 and H6. Five EcR–USP LBD heterodimer structures have been determined by X-ray crystallography to date, along with two structures of isolated monomeric USP LBD domains (reviewed in Hill *et al.*, 2012). In all of the known EcR LBD structures, either an ecdysteroid or a synthetic agonist is completely encapsulated by a pocket made up of residues contributed by helices H3, H5, H6, H7, H11, H12 and the β-sheet; the pocket is closed at one end by the β-sheet and at the other by helix H12 which lies in the 'agonist' conformation on the protein surface, thereby completing a site for binding co-activator proteins (Billas *et al.*, 2003; Carmichael *et al.*, 2005; Renaud & Moras, 2000). In five of the seven known USP LBD structures, this nuclear receptor exhibits a binding pocket containing a phospholipid which appears to act as a structural cofactor. In the remaining two USP structures (subunits of hemipteran and coleopteran ecdysone receptors) the ligand-binding pocket is absent owing to the collapse of elements of the protein structure (Carmichael *et al.*, 2005; Iwema *et al.*, 2007). In all of the published USP structures helix H12 lies in an 'antagonist' conformation. It has been suggested in the case of the *D. melanogaster* USP structure that the LBD is 'locked in an inactive conformation' (Clayton *et al.*, 2001).

By and large, the evidence from structural biology to date has been taken as favouring a hypothesis in which USP, in other than the less derived (*i.e.* non-mecopteran) insect orders, is essentially a constitutive structural partner for EcR without an active hormone-binding role of its own. This model is in stark contrast to that postulated by Jones and coworkers (Jones & Sharp, 1997; Jones, Jones *et al.*, 2013; Jones, Teal *et al.*, 2013). Here, we present two structures of a phthirapteran *Bovicola ovis* ecdysone receptor BoEcR–BoUSP LBD heterodimer derived from crystals obtained in the presence of either an ecdysteroid or the synthetic insecticide methylene lactam (Birru *et al.*, 2010). The former structure displays a canonical ecdysone receptor LBD heterodimer with the EcR subunit enclosing the phytoecdysteroid ponasterone A (PonA) in its binding pocket and with the USP subunit presenting a conformation with no ligand-binding pocket. The conformations of both subunits of the heterodimer observed in the crystals that formed in the presence of the methylene lactam were distinctly different to any observed before for an ecdysone receptor LBD in that both subunits were captured in an open unliganded (*i.e.* apo) state. Strikingly, the conformation of the USP subunit bears a highly significant similarity to that observed in the first nuclear receptor LBD structure to be solved by X-ray diffraction, that of human apo RXR-α (Bourguet *et al.*, 1995), which had an open pocket available for ligand binding.

2. Materials and methods

2.1. Expression and purification of *B. ovis* ecdysone receptor protein

The LBDs of the *B. ovis* heterodimeric ecdysone receptor (BoEcR–BoUSP) were co-expressed using a baculovirus vector and the cells were harvested as described previously (Birru *et al.*, 2010; Graham *et al.*, 2009). Minimal C-terminal segments from BoEcR and BoUSP optimized for crystallography were cloned into a pFastBac Dual vector system (Life Technologies, USA). Baculovirus was generated using standard techniques as per the instruction manual from Invitrogen. Fermentations of Sf21 cells (5.8 l) inoculated with BoEcR-expressing baculovirus were carried out in a Celligen Plus fermentor (New Brunswick). The fermentation was performed at 26°C with 30 rev min^{-1} agitation and was routinely monitored utilizing an automated cell counter (Cedex Hi Res, Roche Innovatis) to determine the cell density, viability and cell size. The culture was harvested at a post-infection time of 72 h by centrifugation at 1500*g* for 10 min at 4°C in a Beckman Avanti J26-XPI centrifuge utilizing a JLA 8.100 rotor. Pellets were snap-frozen in liquid nitrogen and stored at −80°C before protein purification.

The heterodimers, which were expressed as soluble proteins in the cytoplasm of the insect cells, were purified as follows. The cells were thawed, lysed and centrifuged to remove insoluble cell debris. The truncated receptor molecules were engineered to have His_6 affinity tags at the N-terminus of the EcR subunit. Following lysis of the cells, the recombinant protein was isolated by immobilized metal-ion chromatography using Profinity resin (Bio-Rad) in the absence of added ligand. After elution from the resin with 200 m*M* imidazole, the protein was further purified by anion-exchange chromatography (Mono Q; GE Healthcare) and gel filtration (Superdex 200; GE Healthcare). The purified receptor protein showed just the EcR and USP bands on gel electrophoresis (data not shown). The protein was concentrated by ultrafiltration using a Millipore centrifugal concentrator with a 10 kDa cutoff.

2.2. Crystallization and data collection

Ponasterone A (PonA) was added to the protein during the last step of purification for the PonA-bound receptor crystallization trials. To improve the quality of the crystals, the receptor was treated with an excess of *N*-ethylmaleimide (NEM) just prior to the crystallization trials to prevent

multimerization *via* exposed sulfhydryl groups on cysteine residues. Crystallization trials were set up at 20°C in 96-well sitting-drop plates and crystals were found in 20% PEG 3350 with either 0.2 *M* potassium acetate or 0.2 *M* sodium citrate. The concentration of the protein sample was 5.8 or 6.8 mg ml^{-1}, respectively. Crystals were cryoprotected by substituting 10% glycerol plus 10% ethylene glycol for part of the water component of the reservoir conditions and the crystals were cryocooled in the nitrogen stream at the beamline prior to diffraction data collection.

A methylene lactam [SMILES string N#CC1=C(CCCC)-C(N(C2=C(C)C(Cl)=CC=C2)C1=O)=C] was the other compound used in co-crystallization experiments with the purified protein. The sample entering crystallization was at 10 mg ml^{-1} in a buffer consisting of 50 m*M* Tris pH 7.5, 150 m*M* NaCl, 5% glycerol, 5 m*M* DTT, 0.02% azide, 0.37 m*M* methylene lactam. It was mixed in a volume ratio of 1:1 with a crystallization solution consisting of 0.1 *M* bis-tris pH 5.5, 0.1 *M* ammonium sulfate, 17% PEG 10 000 and incubated at 20°C in sitting-drop plates.

Diffraction data sets were collected on the MX1 and MX2 beamlines using a MAR 165 or a Quantum 315 detector, respectively, at the Australian Synchrotron, Melbourne, Australia. Data sets to 2.7 Å resolution were obtained for both a PonA-containing crystal (referred to in the following as the PonA crystal) and a methylene lactam (ML)-containing crystal (the ML crystal). The data were processed with *XDS* (Kabsch, 2010). The obtained *hkl* intensities were input into the *CCP*4 program package for space-group examination, intensity scaling and reduction (Winn *et al.*, 2011). The space group of the PonA crystal was $P4_32_12$ and that of the ML crystal was *C*2. It was observed that the ML crystal quickly suffered radiation damage when exposed to synchrotron radiation. As a result, this data set had a much lower multiplicity than the PonA data set. For data-collection and processing statistics, see Table 1.

Table 1
Data-processing and refinement statistics.

Values in parentheses are for the highest resolution bin.

Crystal (PDB code)	ML (4ozr)	PonA (4ozt)
Data processing		
Space group	*C*2	$P4_32_12$
Unit-cell parameters		
a (Å)	153.7	134.0
b (Å)	42.4	134.0
c (Å)	186.7	95.3
α (°)	90.0	90.0
β (°)	117.7	90.0
γ (°)	90.0	90.0
Resolution (Å)	2.70 (2.85–2.70)	2.70 (2.85–2.70)
No. of observations	33334	295692
Unique reflections	13311	24458
Multiplicity	2.5 (2.5)	12.1 (12.2)
Mean $I/\sigma(I)$	9.1 (2.2)	14.8 (2.7)
Completeness (%)	96.2 (97.7)	100.0 (100.0)
$R_{\rm merge}$†	0.083 (0.480)	0.121 (0.916)
$R_{\rm p.i.m.}$‡	0.063 (0.365)	0.036 (0.271)
Refinement		
$R_{\rm work}/R_{\rm free}$§	0.2239/0.2585	0.1818/0.2171
No. of non-H atoms		
Protein	3123	3517
Ligand	0	42
Solvent	91	61
Average *B* factors (Å^2)		
Protein	56.7	55.6
Ligand¶		44.2
Water	41.3	50.6
R.m.s.d., bond lengths (Å)	0.004	0.005
R.m.s.d., bond angles (°)	1.134	1.418
Ramachandran plot		
Favoured regions (%)	93.5	95.8
Allowed regions (%)	4.7	3.0
Outlier regions (%)	1.8	1.2

† $R_{\rm merge} = \sum_{hkl}\sum_i |I_i(hkl) - \langle I(hkl)\rangle| / \sum_{hkl}\sum_i I_i(hkl)$, where $I_i(hkl)$ is the *i*th observation of reflection intensity and $\langle I(hkl)\rangle$ is the weighted average intensity for multiple and symmetry-related measurements. ‡ Multiplicity-weighted $R_{\rm merge}$ from all reflections. For a definition, see Evans (2006). § 5% of the diffraction data were set aside to calculate the free *R* factor during refinement. ¶ PonA was refined as a fully occupied ligand.

2.3. Structure solution and refinement

The structure of the PonA crystal was solved by molecular replacement with *Phaser* (McCoy *et al.*, 2007) using the structure of the ecdysone receptor LBD heterodimer from the hemipteran *Bemisia tabaci* (PDB entry 1z5x; Carmichael *et al.*, 2005) as the search model. The space group was determined to be $P4_32_12$ during structure solution. Model building was carried out with *Coot* (Emsley *et al.*, 2010) and crystallographic refinement was carried out with *PHENIX* (Adams *et al.*, 2010). Individual *B* factors and TLS refinements were employed at the final stages of crystallographic refinement. After multiple rounds of model building and refinement, the final structure included 433 residues and 61 water molecules, with an $R_{\rm work}$ of 17.9% and an $R_{\rm free}$ of 21.7% at 2.70 Å resolution. PonA was refined as a fully occupied ligand in the structure. The value of the averaged *B* factor for the PonA atoms is lower than that for the protein atoms in the final structure (Table 1).

The structure of the ML crystal was solved by molecular replacement using the structure of the PonA crystal as the search model. A clear solution was obtained with a translation-function *Z*-score (TFZ) of 20.0 (McCoy *et al.*, 2007). Iterative model building and refinement gave a final structure comprising 393 residues and 91 water molecules, with an $R_{\rm work}$ of 22.3% and an $R_{\rm free}$ of 25.8% at 2.70 Å resolution. Calculation of the Ramachandran plot for both the PonA and ML crystal structures revealed favoured backbone dihedral angles for most of the residues, albeit with few outliers. The outlier residues (seven in the structure of the ML crystal and five in that of the PonA crystal) are all located at the edges of the allowed regions in the Ramachandran plot and constitute less than 2% of the total residues in both structures. Refinement statistics are summarized in Table 1.

2.4. Differential scanning fluorimetry (DSF)

Differential scanning fluorimetry (DSF) was performed using the facility at the CSIRO Collaborative Crystallization Centre (http://www.csiro.au/C3) in Melbourne, Australia (Seabrook & Newman, 2013). The final protein concentration of the heterodimer (MW 57 853 Da) in the experiment was 1 µ*M*, which was mixed with PonA or methylene lactam at

molar ratios of 1:0, 1:1, 1:10 and 1:100 of the protein and the compound in a 96-well PCR plate. Each sample was prepared in duplicate with a final volume of 20 µl containing 0.3 µl of a 1:10 dilution of SYPRO Orange dye (Sigma–Aldrich) in Milli-Q water. Stock solutions of PonA and methylene lactam were prepared by dissolving the compounds in ethanol and DMSO, respectively. Lysozyme (0.1 mg ml^{-1}), buffers, protein-omit and ligand-omit solution mixtures in the presence of the 1:10 dye solution were used as controls. The whole experiment was repeated twice from 20 to 100°C at a ramp rate of 6°C min^{-1}.

3. Results and discussion

3.1. The BoEcR–BoUSP LBD structure in crystals formed in the presence of PonA

The BoEcR–BoUSP LBD structure derived from the crystals formed in the presence of PonA is very similar to those of the ecdysone receptor LBD heterodimers from the lepidopteran *Heliothis virescens* (HvEcR–HvUSP; Billas *et al.*, 2003) and the hemipteran *B. tabaci* (BtEcR–BtUSP; Carmichael *et al.*, 2005). Both the EcR and USP LBD subunits display the canonical nuclear receptor fold comprising of 12 α-helices (H1–H12) and a β-sheet between H5 and H6. The helices are organized as a three-layered α-helical sandwich, in which H4, H5, H6, H8 and H9 are in the middle while H1, H2 and H3 are on one side with H7, H10 and H11 on the other (Fig. 1*a*). Structural superposition of BoEcR–BoUSP and BtEcR–BtUSP gave a root-mean-square deviation of 0.87 Å for 419 corresponding C$^{\alpha}$ atoms out of a total of 433, with an overall sequence identity of 78% between the two structures.

PonA is buried in the ligand-binding pocket of the BoEcR subunit, which is enclosed by H3, H5, H6, H7, H10, H12 and the β-sheet (Fig. 1*b*). The interactions between PonA and the protein residues are essentially conserved in the HvEcR, BtEcR and BoEcR structures, including seven hydrogen bonds and extensive hydrophobic interactions (Carmichael *et al.*, 2005). The ligand-binding pocket is sealed at one end by H12, which acts as a lid and forms hydrophobic interactions between Trp516 and the alkyl tail of PonA. The β-sheet seals the opposite end of the pocket, forming hydrophobic interactions involving Phe389 and a hydrogen bond between Ala390 and PonA (Fig. 1*b*).

As in the structure of BtEcR–BtUSP, H12 adopts the agonist conformation in the BoEcR subunit and the antagonist conformation in the BoUSP subunit. Similar conformations have also been observed in all of the other structures of EcR–USP LBD heterodimers that have been determined to date (Billas *et al.*, 2003; Carmichael *et al.*, 2005; Iwema *et al.*, 2007; Browning *et al.*, 2007). The invariant agonist conformation of H12 in the EcR subunit is probably owing to the presence of ecdysteroid (*e.g.* PonA) in the ligand-binding pocket. Since ecdysteroid or other ligands have generally been added during protein purification in order to stabilize the protein for crystallization, no apo structure of EcR LBD has been determined to date. This raised the question of whether H12 may adopt a different conformation with an open binding pocket in the apo state, as observed in the RXR-α apo LBD (Bourguet *et al.*, 1995), or whether the agonist may enter the closed ligand-binding pocket *via* a solvent channel, as observed in the oestrogen receptor and other steroid receptors (Nettles *et al.*, 2008), with only minor structural disturbance.

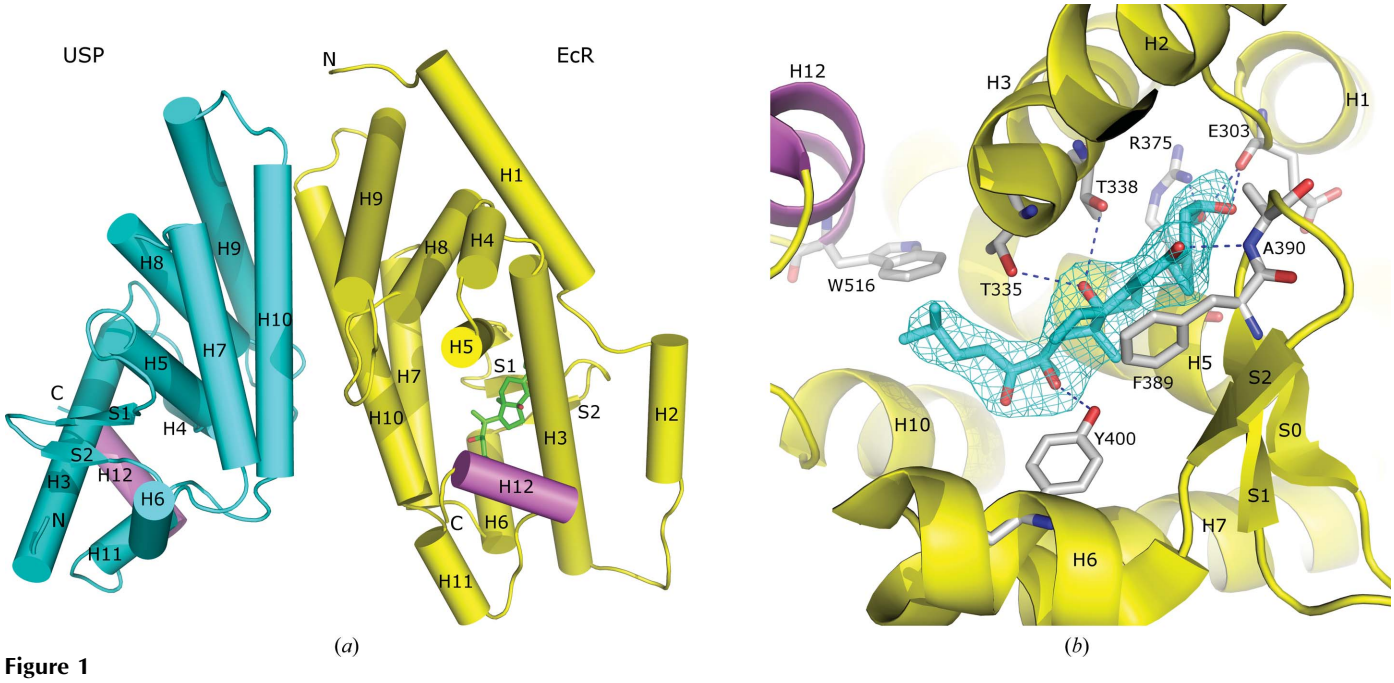

Figure 1
(*a*) The structure of the *B. ovis* ecdysone receptor LBD heterodimer in a crystal formed in the presence of PonA. PonA in the pocket of the EcR subunit is shown in stick representation. H12 is coloured violet. (*b*) Details of the binding of PonA (aqua-coloured backbone) within the ligand-binding pocket of the EcR subunit. A difference OMIT map is shown which is contoured at the 3.5σ level. Hydrogen-bonding interactions are shown as broken lines. The structural figures in this communication were produced using *PyMOL* (Schrödinger).

The interactions of H12 with the other parts of the protein are mainly hydrophobic in both the BoEcR and BoUSP subunits. The buried interface area is about 487 Å^2 for H12 in the EcR subunit and 672 Å^2 in the USP subunit. A hydrogen bond is found between the NE1 atom of Trp516 in H12 and the OG atom of Ser369 in the EcR subunit, while a salt bridge is formed between the OD1 atom of Asp381 in H12 and the NH1 atom of Arg235 in the USP subunit. It can be inferred that H12 is more tightly packed on the protein surface in the USP subunit than in the EcR subunit because of a larger contact interface.

3.2. The BoEcR–BoUSP LBD structure in crystals formed in the presence of a methylene lactam

During screening of a chemical library for new ligands for the *B. ovis* ecdysone receptor, methylene lactams were identified as a new class of compounds that showed high inhibitory effects on the binding of a fluorescein–ecdysteroid adduct to the receptor (Birru *et al.*, 2010). To investigate how the methylene lactams interact with the receptor, structure determination was carried out on the BoEcR–BoUSP heterodimer LBD crystallized in the presence of a member of this chemical class (see §2). The refined structure is, in its general features, similar to that of the PonA crystal, which was used as the search model in molecular replacement (Fig. 2*a*). Superposition of the two structures gave a root-mean-square deviation of 1.06 Å for 324 corresponding C$^\alpha$ atoms out of a total of 433 (Fig. 2*b*).

Although the crystal was grown in the presence of the methylene lactam, no clear density could be allocated to the compound in the refined structure, suggesting that the compound was either disordered or not bound in the structure. One major feature of the refined structure is that some regions constituting the ligand-binding pocket of the EcR subunit were not visible in the electron-density map, which included residues 310–327 and 389–406. These two regions encompass residues from the C-terminal part of H2 to the N-terminal part of H3 and from the C-terminal part of β1 to the N-terminal part of H7, including the entire β2 and H6 secondary structures. The poorly defined polypeptide segments in the vicinity of the canonical ligand-binding pocket could be induced by the methylene lactam, reflecting considerable conformational flexibility of the EcR subunit. It was previously shown that the ligand-binding pocket of the EcR LBD may display extreme conformational flexibility and adaptability when binding to structurally different ligands (Billas *et al.*, 2003).

A conspicuous feature of the structure in the ML crystal is the conformational change of H12 in both subunits of the heterodimer (Fig. 2*b*). Instead of H12 exhibiting the agonist conformation, as in the EcR subunit structure of the crystal containing PonA, the residues after H11 in the EcR subunit of the ML crystal form an extended polypeptide chain which makes a U-turn after residue 509. Concomitantly, H12 of the EcR subunit unwinds and the ligand-binding pocket region is opened (Fig. 2*a*). In the USP subunit, H11 and H12 extend on the protein surface after H10 and, unlike their conformation in the PonA crystal, do not make the turn to form the antagonist conformation (Figs. 2*a* and 2*b*). The USP structure in particular is strikingly similar to the apo form of RXR-α LBD (Bourguet *et al.*, 1995). Structural superposition of the two structures gave a root-mean-square deviation of 1.35 Å for 179 corresponding C$^\alpha$ atoms out of a total of 196. The conformations of H12 in the two subunits of the ML crystal have not

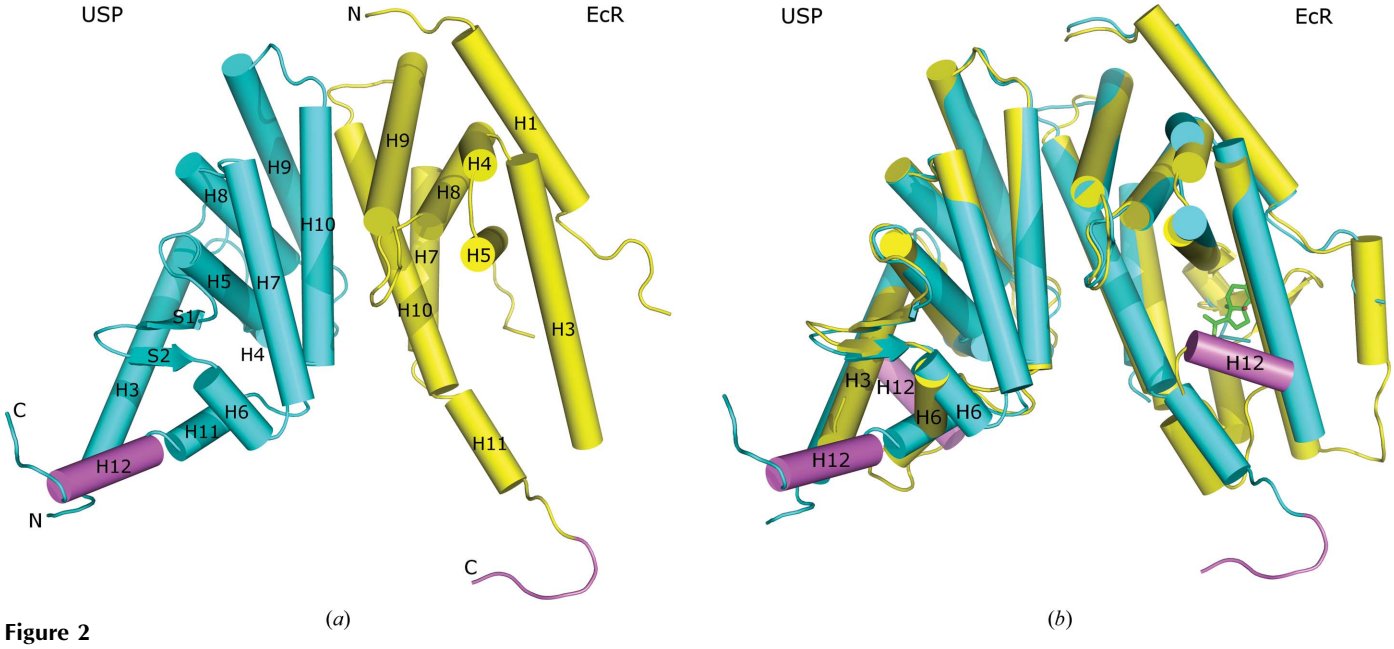

Figure 2
(*a*) The structure of the *B. ovis* ecdysone receptor LBD heterodimer in a crystal formed in the presence of ML. H12 in the USP subunit and the region corresponding to H12 in the PonA crystal of the EcR subunit are coloured violet. (*b*) Structural superposition of the BoEcR–BoUSP heterodimer of the PonA crystal (yellow) with that of the ML crystal (cyan). PonA in the ligand-binding pocket of the PonA crystal is shown in stick representation. H12, or the region originally corresponding to H12, is coloured violet.

been observed in previous ecdysone receptor LBD heterodimer structures. It is also the first time that USP has been found to be able to adopt an open conformation like the apo form of RXR-α LBD. The conformational change of H12 is concerted with a number of structural variations in the two subunits, which are described in more detail below.

3.3. Comparison of the EcR subunit conformations

Superposition of the EcR subunit of the ML crystal with that of the PonA crystal gave a root-mean-square deviation of 0.95 Å for 166 corresponding C^{α} atoms out of a total of 238. As mentioned above, a number of residues were not visible in the ML crystal owing to poor density. While residues 306–315 form H2 in the structure of the PonA crystal, only residues 306–309 are visible in the structure of the ML crystal, and these adopt an extended conformation instead of a helix. The loop connecting H2 and H3 and the N-terminal part of H3 including residues 322–327 are also missing in the structure of the ML crystal. In concert with the conformational change at the C-terminus of the EcR subunit in the ML crystal, the N-terminal part of H3, including residues 328–340, is tilted towards the space that was previously occupied by H12 and the loop connecting H11 and H12 in the PonA crystal (Figs. 3*a* and 3*b*). The tilt of H3 also seems to provide space for the missing residues after 386–388. Residues 386–388 adopt an extended conformation pointing towards the helix. Residues 386–389 form strand S1 in the structure of the PonA crystal. While residues 386–388 are visible in the structure of the ML crystal, the subsequent residues corresponding to S2 and H6 are missing in the structure of the ML crystal.

The C-terminal helix H12 in the ligand-binding domain of nuclear receptors may act as a ligand-dependent transcriptional switch that closes off the ligand-binding pocket upon taking up agonist ligands (Renaud & Moras, 2000). In the RXR-α apo structure, helix H10 is followed by a short kinked helix H11 and then continued by H12, forming an extended conformation at the C-terminus (Bourguet *et al.*, 1995; Fig. 3*c*). Upon binding agonists, however, the polypeptide chain after H10 makes a U-turn and H12 switches to the agonist conformation by running roughly antiparallel to H10, forming a more compact structure (Renaud & Moras, 2000). H12 in the EcR subunit of the structure of the PonA crystal displays the typical agonist conformation (Fig. 3*a*), while the C-terminus of the EcR subunit of the ML crystal is displaced outwards from the core of the protein to give an apo conformation with an open ligand-binding pocket (Fig. 3*b*). How this conformational change is induced is still not clear, but it provides the first evidence that the C-terminal end of the EcR subunit can adopt dramatic conformational changes as observed in ligand-binding domains of other nuclear receptors (Nolte *et al.*, 1998; Renaud & Moras, 2000). The structural adjustment and

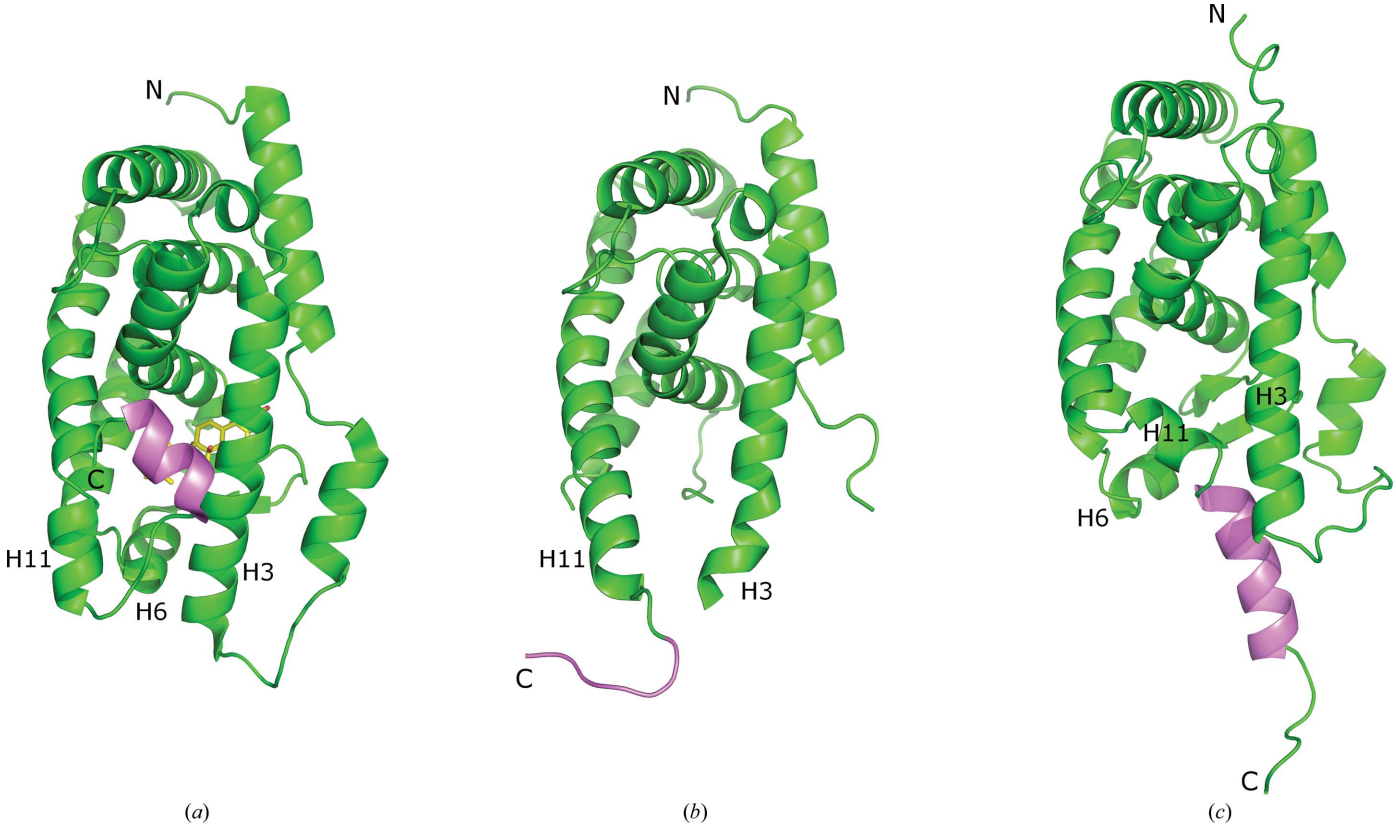

Figure 3
Comparison of (*a*) the EcR subunit structure of the PonA crystal, (*b*) the EcR subunit structure of the ML crystal and (*c*) the retinoic acid receptor α (RXR-α) apo LBD structure (Bourguet *et al.*, 1995; PDB entry 1lbd). PonA in the ligand-binding pocket is shown in stick representation. The structures are aligned in the same orientation. H12, or the region originally corresponding to H12, is coloured violet.

opening up of the ligand-binding pocket may well facilitate the initial steps in the binding of small-molecule ligands.

3.4. Comparison of the USP subunit conformations

USP (ultraspiracle) is a homologue of the mammalian retinoid X receptor (RXR). There are still open questions relating to the roles of USP in different insect orders and the search for its natural ligands is ongoing. In the meantime, USP has often been considered a 'silent partner' in the heterodimer with the various EcR subunits (Iwema *et al.*, 2007). Invariably, the structures of USP LBDs that have been solved to date display the so-called inactive antagonist conformation, with helix H12 packed on the protein surface outside H3 and H4, whether the subunit was crystallized alone or in complex with EcR LBD (Clayton *et al.*, 2001; Billas *et al.*, 2001, 2003; Carmichael *et al.*, 2005; Iwema *et al.*, 2007; Browning *et al.*, 2007; Figs. 4*a* and 4*c*). A hydrophobic pocket was found in the USP LBD of *D. melanogaster* and *H. virescens*. Phospholipids that were probably derived from the bacterial expression hosts were bound in the pocket (Clayton *et al.*, 2001; Billas *et al.*, 2001; Browning *et al.*, 2007). The question of whether or not the pocket represents a functional hormone-binding site for USP LBDs across different insect orders remains the subject of investigation and some controversy. We have not observed a pocket in the USP subunit structure of the PonA-bound BoEcR–BoUSP LBD crystals; this is consistent with the previously observed USP subunit structures from *B. tabaci* and *Tribolium castaneum*, where the pocket is absent owing to the 'folding in' of the regions connecting H6 to H7 and H10 to H12 (Carmichael *et al.*, 2005; Iwema *et al.*, 2007). It should be noted that residues prior to H3 were not observed in the USP subunits of *B. ovis* or *B. tabaci*, which were expressed in insect cells, while they were observed in the others mentioned above, which were expressed in *E. coli*. Although the loop connecting H1 and H3 was initially suggested to be important to maintain the antagonist conformation of H12 in the USP LBD of *D. melanogaster* and *H. virescens* (Clayton *et al.*, 2001; Billas *et al.*, 2001), it was subsequently shown to be flexible. Since it can adopt a different conformation without influencing H12 in the USP LBD of *T. castaneum*, it seems that H1 is dispensable (Iwema *et al.*, 2007).

While the BoUSP subunit conformation observed in the PonA crystal is very similar to those of *T. castaneum* and *B. tabaci* USP, the structure of the ML crystal reveals unexpected conformational changes, particularly at the C-terminus, where H12 adopts an apo-like conformation that has only been observed previously in RXR-α LBD (Figs. 4*b* and 3*c*). Superposition of the USP subunit of the ML crystal with that of the PonA crystal gave a root-mean-square deviation of 1.11 Å for 159 corresponding C^{α} atoms out of a total of 196. In concert with the structural change of H12 from the antagonist conformation to an apo-like conformation in the ML crystal, helices H3 and H6 have shifted apart in order to give space to H11 and H12, which are positioned between them (Figs. 4*a* and 4*b*). The C-terminal end of H6 is reorientated outwards to the protein surface by a rotation of about 40°, which is accompanied by a conformational change of residues 275–277 from a loop (the 'folding-in' region) to the first helix turn of H7 (Figs. 4*a* and 4*b*). As a result, an open pocket is revealed for the first time, which has a size of about 11 Å in width and 12 Å in depth with an approximate volume of 700 $Å^3$ (Figs. 5*a* and 5*b*). It is enclosed by H3, H5, H10, H11 and H12 with strands S1 and S2 at the bottom.

The position of the pocket is very similar to that of the ligand-binding pocket of the EcR subunit as observed in the

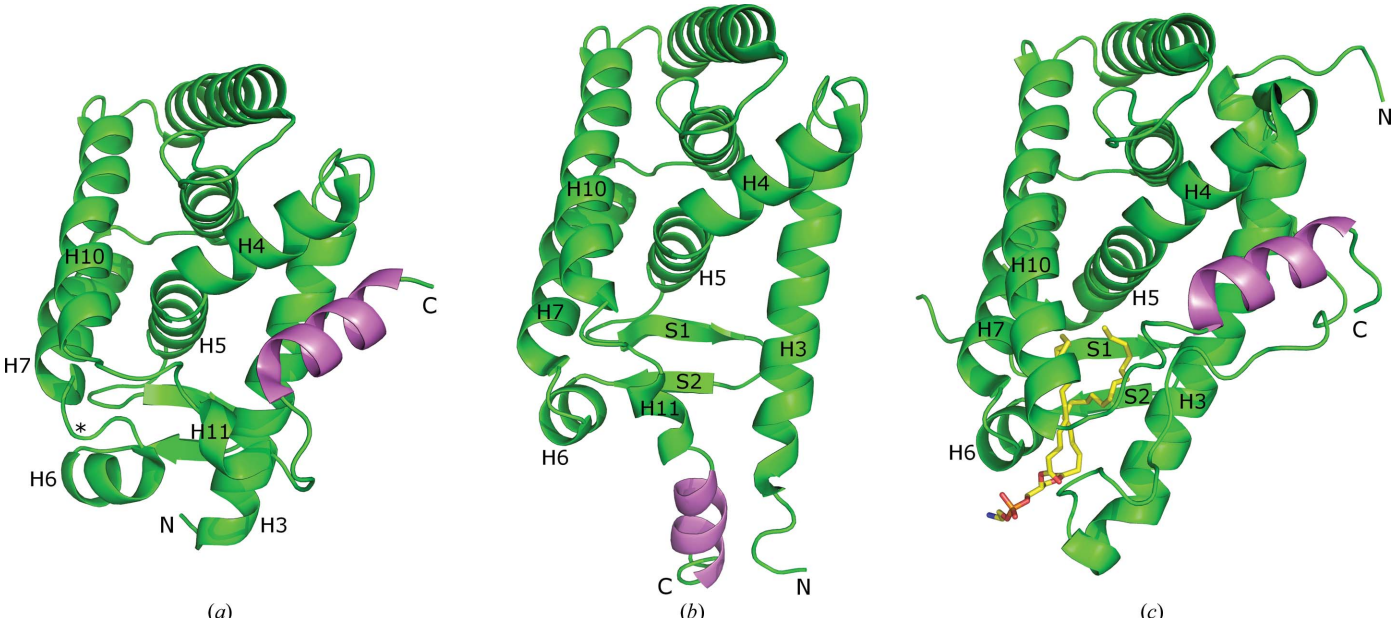

Figure 4
The USP structure of (*a*) the PonA BoEcR–BoUSP crystal, (*b*) the ML BoEcR–BoUSP crystal and (*c*) the *H. virescens* USP monomer (Billas *et al.*, 2001; PDB entry 1g2n). The asterisk in (*a*) indicates the region of residues 275–277. The bound phospholipid is shown in stick representation in (*c*). The structures are aligned in the same orientation. H12 is coloured violet.

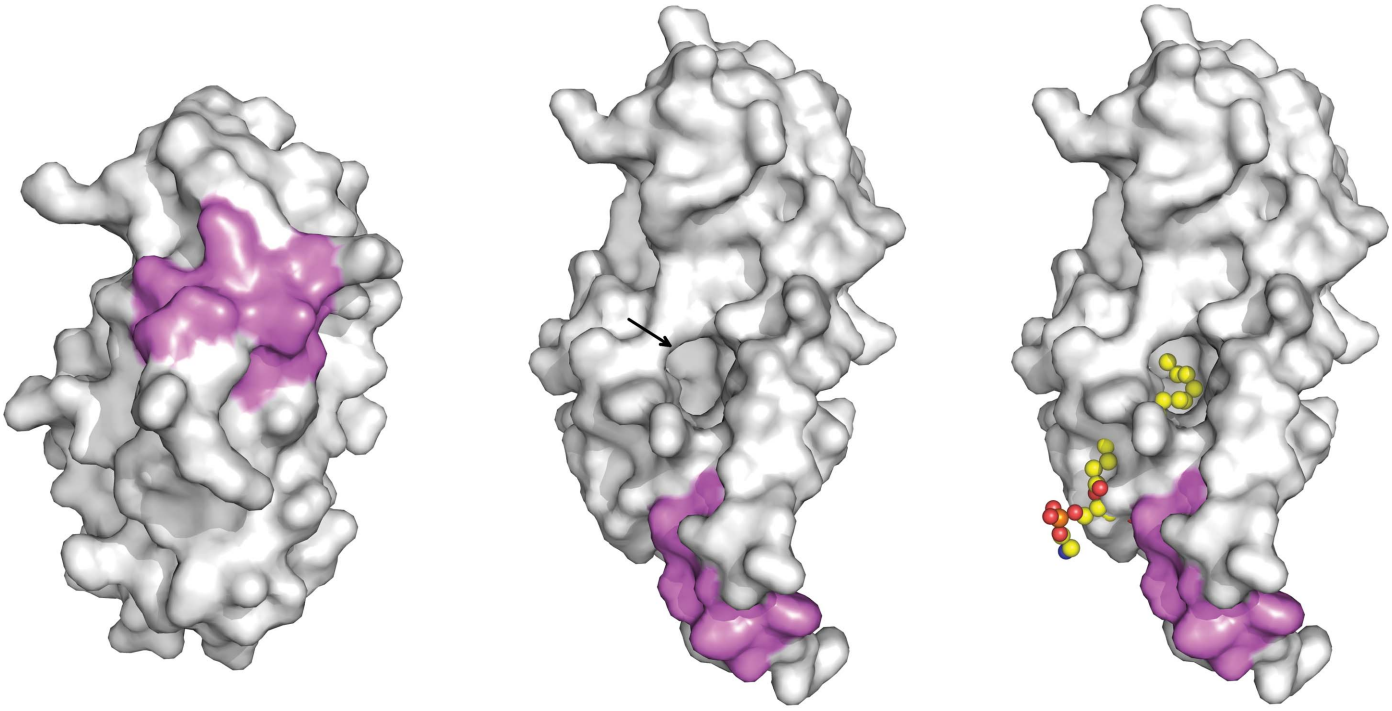

(*a*) (*b*) (*c*)

Figure 5
Surface representation of the BoUSP subunit structure of (*a*) the PonA crystal, (*b*) the ML crystal and (*c*) the ML crystal aligned with the phospholipid (in sphere representation) from the *H. virescens* USP structure (Billas *et al.*, 2001; PDB entry 1g2n). The H12 region is coloured violet. The arrow in (*b*) indicates the open ligand-binding pocket.

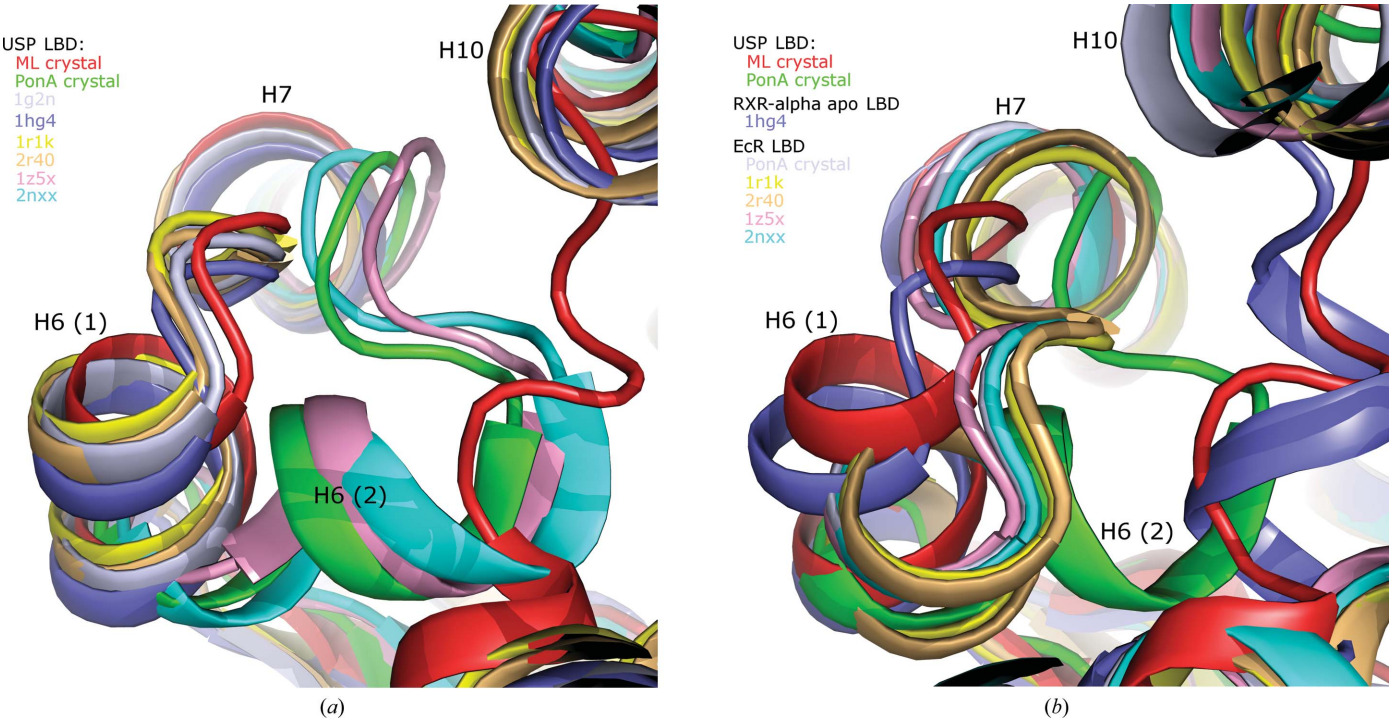

(*a*) (*b*)

Figure 6
The different orientations of BoUSP H6, represented by H6(1) for the subunit in the ML crystal and H6(2) for that in the PonA crystal. (*a*) Superposition of the USP subunit structures. Those with bound phospholipids have H6 adopting the H6(1) orientation, as in the ML crystal, and include the structures of PDB entries 1g2n, 1hg4, 1r1k and 2r40. Those with no bound ligand adopt the H6(2) orientation, as in the PonA crystal, and include PDB entries 1z5x and 2nxx. (*b*) Superposition of the BoUSP subunit structures of the ML and PonA crystals with the retinoic acid receptor α (RXR-α) apo LBD (PDB entry 1hg4) and various EcR LBD structures, including PDB entries 1r1k, 2r40, 1z5x and 2nxx and the BoEcR subunit of the PonA crystal. In RXR-α apo LBD and in all EcR LBDs, H6 resembles H6(1) (*i.e.* the conformation found in the USP subunit of the ML crystal) more closely than H6(2).

PonA crystal and other EcR LBD structures. Similarly, the internal surface of the pocket is predominantly hydrophobic, reflecting the presence of aromatic residues including Trp238, Phe246 and Phe372. The pocket runs roughly perpendicular to the phospholipid-binding pocket found in mecopteran USPs and partially overlaps with it, while the latter has its opening on the other side of H10 (Clayton *et al.*, 2001; Billas *et al.*, 2001). To illustrate the difference, the phospholipid bound in the pocket of *H. virescens* USP (Billas *et al.*, 2001) is aligned onto the *Bo*USP structure of the ML crystal and is shown in Fig. 5(*c*). Comparison with the USP subunit structure of the PonA crystal indicates that the creation of this new open pocket in the ML crystal is mainly owing to local structural adjustments, especially the reorientation of H6 and the following loop between H6 and H7. In the PonA structure, the pocket was filled by residues from H5, H11 and the loop connecting H6 and H7, including Phe246, Val275, Ile278 and Phe370.

It is interesting to note that among all of the other USP structures solved to date, those with bound phospholipids have H6 and the following loop orientated in the same manner as in the ML crystal, whereas the others with no bound ligand adopt the same orientation as in the PonA crystal (Fig. 6*a*). Similarly, in all of the EcR LBD structures solved to date, including that in the PonA crystal reported here, as well as in the RXR-α apo LBD structure, H6 and the following loop adopt a conformation more closely resembling that in the USP structure of the ML crystal (Fig. 6*b*). As H6 participates in the formation of the ligand-binding pocket in the EcR LBD and the phospholipid-binding pocket in the USP LBD, its reorientation seems necessary to allow the binding of ligands. The flexibility of H6 was also illustrated in the EcR subunit structure of the ML crystal, where it was not visible in the electron density, together with a number of other residues constituting the ligand-binding pocket, as described above. It is possible that these structural changes, including the flip of H12, in the USP subunit structure of the ML crystal were induced by the methylene lactam, although it is not visible in the electron-density maps.

Taken together, the structural comparisons suggest that the USP LBD may undergo conformational change from a closed state (as in the PonA crystal) to an open state (as in the ML crystal), possibly to ready the protein for ligand binding. This discovery may provide a new starting point for deciphering a ligand-binding function for the USP LBD and searching for natural ligands, at least in some insect orders. It may be of interest that the size of the pocket in BoUSP is sufficient to accommodate potential ligands other than phospholipids, including juvenile hormone III or methyl farnesoate. Jones, Teal *et al.* (2013) reported that three residues (Gln288, Leu366 and Asn325) that participate in the formation of the ligand-binding pocket in DmUSP are necessary for high-affinity binding of methyl farnesoate and activity *in vivo*. Structural alignment of BoUSP with DmUSP indicates that corresponding residues in BoUSP contribute to the formation of the new open pocket, with two of them being conserved (Gln208 and Leu259) and Asn325 replaced by Ala245.

3.5. Methylene lactam decreases the thermal stability of the BoEcR–BoUSP heterodimer

The question of whether the unexpected conformational changes in the BoEcR–BoUSP LBD structure in the ML crystal were owing to crystallization artefacts prompted us to perform a differential scanning fluorimetry (DSF) study to investigate the interactions of the heterodimer with PonA and

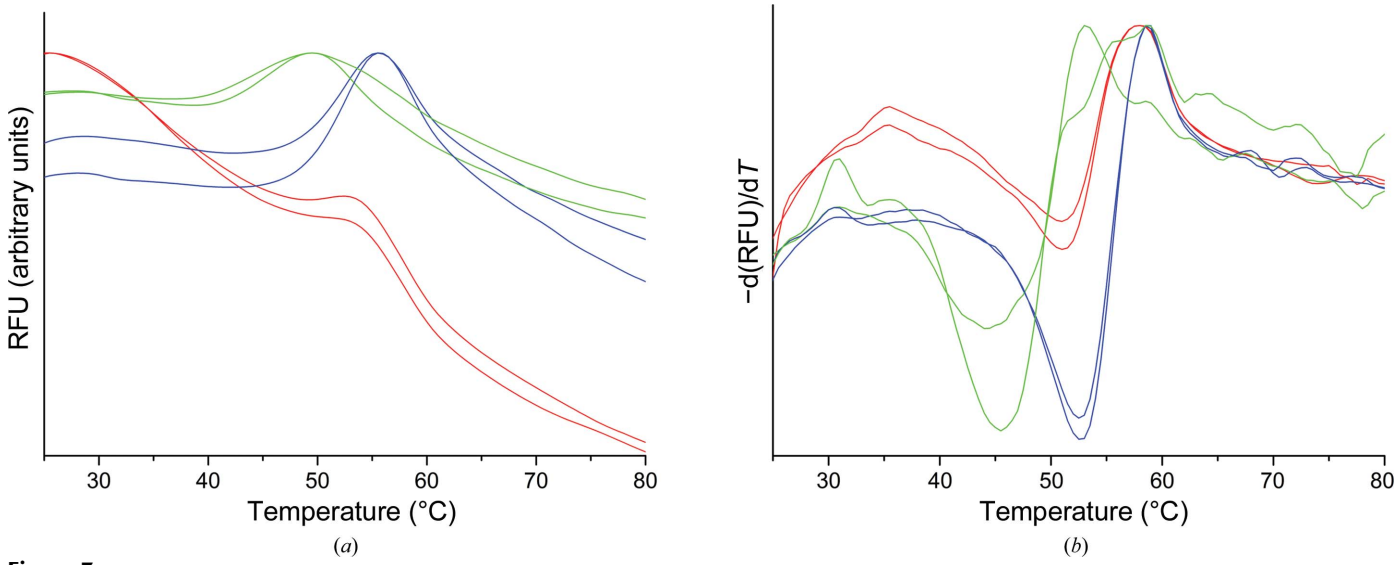

Figure 7
Melting curves of the DSF experiment, showing (*a*) the fluorescence responses (relative fluorescence units; RFU) and (*b*) the first derivatives of the melting curves [−d(RFU)/d*T*]. The negative peak of the first derivative is a good approximation of the temperature of hydrophobic exposure (T_h). BoEcR–BoUSP was mixed with PonA or methylene lactam in a molar ratio of 1:100. Experiments with ratios of 1:1 and 1:10 that are not shown in the figure displayed similar and consistent results. The values for T_h of the heterodimer are 51.0°C for protein only (red), 45.0°C with methylene lactam (green) and 52.5°C with PonA (blue). Duplicate samples were prepared in the experiment, which was repeated twice.

the methylene lactam in solution. Consistent results were observed among the different ratios used to mix the protein with the compounds, as described in §2. While the mixture of the protein with PonA slightly increased the temperature of hydrophobic exposure (T_h) of the heterodimer, methylene lactam dramatically decreased it by about 6°C (Fig. 7). It has been shown that T_h is in good correlation with the melting temperature of proteins (T_m; He *et al.*, 2010). The binding of PonA led to a more stable structure, consistent with the PonA crystal structure, in which the hormone effectively fills the predominantly hydrophobic major pocket in EcR, and the fact that the presence of an ecdysteroid ligand such as PonA stabilizes the protein during purification (Graham, Pilling *et al.*, 2007) and facilitates crystallization. The destabilizing effect of methylene lactam is consistent with the observation in the ML crystal structure that more hydrophobic surfaces are exposed as a result of the conformational changes, such as those involving H12 and H6, and these would be expected to facilitate the thermal unfolding of the protein. From a biophysical point of view, the conformational change of H12 in the structure of the ML crystal can be considered as a partial unfolding of the protein. Whether methylene lactam in solution would cause exactly the same conformational changes as observed in the BoEcR–BoUSP crystal will require further investigation. However, the destabilizing effect of the methylene lactam on the higher order structure of the protein is obvious in solution, as demonstrated by the DSF data.

4. Concluding remarks

The differences between the BoEcR–BoUSP heterodimer LBD structures observed in the presence of PonA or ML clearly illustrate the considerable conformational flexibility that both the EcR and USP LBDs can exhibit. Helix H12, which lies on the surface of both subunits, is probably one of the most flexible regions, and can evidently flip to open the ligand-binding pockets of both EcR and USP. This may be indicative that the LBDs of the ecdysone receptor subunits can undergo conformational changes from an apo form to the agonist/antagonist form upon the binding of ligands, similar to those observed in the LBD of RXR-α and other nuclear receptors. The effect of the methylene lactam on the BoEcR–BoUSP LBD is distinctive: it decreases the thermal stability of the heterodimer in solution and induces dramatic conformational changes in the crystal structure. As the methylene lactam is not visible in the electron-density map of the structure, the nature of its interaction with the heterodimer remains unclear. Its ability to cause displacement of the ecdysteroid–fluorescein conjugate in the receptor-binding assay (Birru *et al.*, 2010) may be at least partially owing to its ability to induce opening of the EcR ligand-binding pocket.

It was surprising to find that H12 of the USP subunit can adopt an apo-like conformation in the crystal formed in the presence of a methylene lactam, a conformation resembling that of the first nuclear receptor LBD to be solved by X-ray diffraction, apo RXR-α (Bourguet *et al.*, 1995). This new structure clearly indicates that H12 in a USP LBD can extend outwards in an apo conformation that displays an open ligand-binding pocket. Such conformational flexibility suggests that, at least in the order Phthiraptera, USP is probably not deadlocked in an antagonist conformation to prevent it from undergoing allosteric changes, as previously suggested (Clayton *et al.*, 2001; Iwema *et al.*, 2007). The fact that H12 can adopt open conformations at the same time in both EcR and USP subunits is unique amongst all of the heterodimeric EcR–USP structures solved to date and may be significant for further studies of their central biological functions. The revelation of an unoccupied pocket in the USP subunit structure tends to diminish structural biological arguments against the possibility of functional ligand–protein interactions for USP and could be helpful in the search for potential ligands for USP LBDs.

We thank the staff of the MX1 and MX2 beamlines of the Australian Synchrotron for their help in data collection and the CSIRO Collaborative Crystallization Centre in Melbourne, Australia for crystallization and DSF experiments. Support from Australian Wool Innovation Ltd and DuPont Crop Protection is gratefully acknowledged.

References

Adams, P. D. *et al.* (2010). *Acta Cryst.* D**66**, 213–221.
Billas, I. M. L., Iwema, T., Garnier, J.-M., Mitschler, A., Rochel, N. & Moras, D. (2003). *Nature (London)*, **426**, 91–96.
Billas, I. M. L., Moulinier, L., Rochel, N. & Moras, D. (2001). *J. Biol. Chem.* **276**, 7465–7474.
Birru, W. *et al.* (2010). *Bioorg. Med. Chem.* **18**, 5647–5660.
Bourguet, W., Ruff, M., Chambon, P., Gronemeyer, H. & Moras, D. (1995). *Nature (London)*, **375**, 377–382.
Browning, C., Martin, E., Loch, C., Wurtz, J.-M., Moras, D., Stote, R. H., Dejaegere, A. P. & Billas, I. M. L. (2007). *J. Biol. Chem.* **282**, 32924–32934.
Butenandt, A. & Karlson, P. (1954). *Z. Naturforsch. B*, **9b**, 389–391.
Carmichael, J. A., Lawrence, M. C., Graham, L. D., Pilling, P. A., Epa, V. C., Noyce, L., Lovrecz, G., Winkler, D. A., Pawlak-Skrzecz, A., Eaton, R. E., Hannan, G. N. & Hill, R. J. (2005). *J. Biol. Chem.* **280**, 22258–22269.
Clayton, G. M., Peak-Chew, S. Y., Evans, R. M. & Schwabe, J. W. (2001). *Proc. Natl Acad. Sci. USA*, **98**, 1549–1554.
Dhadialla, T. S., Carlson, G. R. & Le, D. P. (1998). *Annu. Rev. Entomol.* **43**, 545–569.
Emsley, P., Lohkamp, B., Scott, W. G. & Cowtan, K. (2010). *Acta Cryst.* D**66**, 486–501.
Evans, P. (2006). *Acta Cryst.* D**62**, 72–82.
Graham, L. D., Johnson, W. M., Pawlak-Skrzecz, A., Eaton, R. E., Bliese, M., Howell, L., Hannan, G. N. & Hill, R. J. (2007). *Insect Biochem. Mol. Biol.* **37**, 611–626.
Graham, L. D., Johnson, W. M., Tohidi-Esfahani, D., Pawlak-Skrzecz, A., Bliese, M., Lovrecz, G. O., Lu, L., Howell, L., Hannan, G. N. & Hill, R. J. (2009). *Ecdysone: Structures and Functions*, edited by G. Smagghe, pp. 447–474. Dordrecht: Springer.
Graham, L. D., Pilling, P. A., Eaton, R. E., Gorman, J. J., Braybrook, C., Hannan, G. N., Pawlak-Skrzecz, A., Noyce, L., Lovrecz, G. O., Lu, L. & Hill, R. J. (2007). *Protein Expr. Purif.* **53**, 309–324.
He, F., Hogan, S., Latypov, R. F., Narhi, L. O. & Razinkov, V. I. (2010). *J. Pharm. Sci.* **99**, 1707–1720.
Hill, R. J., Billas, I. M. L., Bonneton, F., Graham, L. D. & Lawrence, M. C. (2013). *Annu. Rev. Entomol.* **58**, 251–271.
Hill, R. J. *et al.* (2012). *Adv. Insect Physiol.* **43**, 299–351.

Horn, D. H. S. & Bergamasco, R. (1985). *Comprehensive Insect Physiology, Biochemistry and Pharmacology*, edited by G. A. Kerkut & L. Gilbert, pp. 185–248. Oxford: Pergamon Press.
Hu, X., Cherbas, L. & Cherbas, P. (2003). *Mol. Endocrinol.* **17**, 716–731.
Iwema, T., Billas, I. M. L., Beck, Y., Bonneton, F., Nierengarten, H., Chaumot, A., Richards, G., Laudet, V. & Moras, D. (2007). *EMBO J.* **26**, 3770–3782.
Jindra, M., Palli, S. R. & Riddiford, L. M. (2013). *Annu. Rev. Entomol.* **58**, 181–204.
Jones, D., Jones, G. & Teal, P. E. (2013). *Gen. Comp. Endocrinol.* **194**, 326–335.
Jones, G. & Sharp, P. A. (1997). *Proc. Natl Acad. Sci. USA*, **94**, 13499–13503.
Jones, G., Teal, P., Henrich, V. C., Krzywonos, A., Sapa, A., Wozniak, M., Smolka, J. & Jones, D. (2013). *Gen. Comp. Endocrinol.* **182**, 73–82.
Kabsch, W. (2010). *Acta Cryst.* D**66**, 125–132.
Karlson, P. (1956). *Vitam. Horm.* **14**, 227–266.
Koelle, M. R., Talbot, W. S., Segraves, W. A., Bender, M. T., Cherbas, P. & Hogness, D. S. (1991). *Cell*, **67**, 59–77.
McCoy, A. J., Grosse-Kunstleve, R. W., Adams, P. D., Winn, M. D., Storoni, L. C. & Read, R. J. (2007). *J. Appl. Cryst.* **40**, 658–674.
Nakagawa, Y. (2005). *Vitam. Horm.* **73**, 131–173.
Nettles, K. W., Bruning, J. B., Gil, G., Nowak, J., Sharma, S. K., Hahm, J. B., Kulp, K., Hochberg, R. B., Zhou, H., Katzenellenbogen, J. A., Katzenellenbogen, B. S., Kim, Y., Joachmiak, A. & Greene, G. L. (2008). *Nature Chem. Biol.* **4**, 241–247.
Nolte, R. T., Wisely, G. B., Westin, S., Cobb, J. E., Lambert, M. H., Kurokawa, R., Rosenfeld, M. G., Willson, T. M., Glass, C. K. &. Milburn, V. A. (1998). *Nature (London)*, **395**, 137–143.
Nowickyj, S. M., Chithalen, J. V., Cameron, D., Tyshenko, M. G., Petkovich, M., Wyatt, G. R., Jones, G. & Walker, V. K. (2008). *Proc. Natl Acad. Sci. USA*, **105**, 9540–9545.
Renaud, J.-P. & Moras, D. (2000). *Cell. Mol. Life Sci.* **57**, 1748–1769.
Seabrook, S. A. & Newman, J. (2013). *ACS Comb. Sci.* **15**, 387–392.
Thomas, H. E., Stunnenberg, H. G. & Stewart, A. F. (1993). *Nature (London)*, **362**, 471–475.
Wing, K. D., Slawecki, R. A. & Carlson, G. R. (1988). *Science*, **241**, 470–472.
Winn, M. D. *et al.* (2011). *Acta Cryst.* D**67**, 235–242.
Yao, T.-P., Forman, B. M., Jiang, Z., Cherbas, L., Chen, J.-D., McKeown, M., Cherbas, P. & Evans, R. M. (1993). *Nature (London)*, **366**, 476–479.
Yao, T.-P., Segraves, W. A., Oro, A. E., McKeown, M. & Evans, R. M. (1992). *Cell*, **71**, 63–72.